

## Squeezed states in phase-sensing interferometers

Roy S. Bondurant

*Massachusetts Institute of Technology, Lincoln Laboratory, P.O. Box 73, Lexington, Massachusetts 02173*

Jeffrey H. Shapiro

*Department of Electrical Engineering and Computer Science, Massachusetts Institute of Technology, Cambridge, Massachusetts 02139*

(Received 31 October 1983)

The performance of phase-sensing interferometers employing squeezed states and homodyne detection is analyzed and compared to the performance of systems employing direct detection. Standard differenced direct-detection Michelson and Mach-Zehnder interferometers are shown to be suboptimal in the sense that an observation/measurement-noise coupling occurs, which can degrade performance. Homodyne-detection interferometers in which the phase shift in one arm is the conjugate of that in the other arm do not suffer from the preceding drawback. Overall, however, the performance of differenced direct-detection and homodyne-detection interferometers is similar in single-frequency operation. In particular, both detection schemes reach the standard quantum limit on position-measurement sensitivity in single-frequency interferometric gravity-wave detectors at roughly the same average photon number. This limit arises from back action in the form of radiation pressure fluctuations entering through the energy-phase uncertainty principle. Multifrequency devices can circumvent this uncertainty principle, as illustrated by the conceptual design given for a two-frequency interferometer which can greatly surpass the standard quantum limit on position sensing. This configuration assumes that ideal photodetectors respond to photon flux rather than energy flux.

### I. INTRODUCTION

The use of squeezed states in a single-frequency Michelson interferometer gravity-wave detector was considered by Caves,<sup>1</sup> who showed that a squeezed-state interferometer requires substantially fewer photons than does a conventional coherent-state interferometer to reach the standard quantum limit (SQL) on position-measurement accuracy. Caves's analysis dealt in detail only with direct-detection (photon counting) methods, whereas it is known that optical homodyne detection of squeezed states generally provides a higher signal-to-noise ratio (SNR) than does direct detection. Moreover, a minimum-uncertainty squeezed state is the optimum state to use with homodyne detection, as it yields the highest SNR of any state for this detection format.<sup>2</sup> The present study began as a search for the further reduction in the number of photons required to achieve the SQL that might be realized with the use of homodyne detection in a squeezed-state interferometer. As will be described, a number of surprises ensued in this quest. In particular, it will be shown that homodyne detection offers no significant advantage in a single-frequency squeezed-state interferometer, but heterodyne detection in a multifrequency squeezed-state interferometer permits the SQL to be surpassed by a large margin.

The paper is organized as follows. Section II briefly reviews some now well-known results from quantum optics concerning single-mode squeezed states and various means for detecting them. This section will establish notation and exhibit the large SNR advantage that homodyne detection has over direct detection with single-mode

squeezed states. In Sec. III, single-frequency phase-sensing interferometers will be considered with respect to their quantum-state input/output relations. It will be shown that there is an optimum interferometer design which results in minimum-uncertainty squeezed states being produced at the output ports when they are present at the input ports of the system. The standard Michelson and Mach-Zehnder configurations *do not* fall into this category. What is needed is a phase-conjugate interferometer in which the phase shift incurred in one arm is the conjugate of that incurred in the other arm.

Section IV applies the results of Sec. III to single-frequency gravitational-wave detectors. Here it will be shown that a single-frequency squeezed-state homodyne-detection interferometer achieves SQL position-sensing performance with basically the same photon-number requirement as Caves's direct-detection interferometer. This equivalence in performance is reconciled with the homodyne advantage found in Sec. II by arguing that Caves's interferometer is exploiting nonclassical correlations between the fields in the two output ports through his differenced-detector arrangement.

The results of Sec. IV are consistent with the previously held view<sup>1</sup> that back action, in the form of radiation pressure fluctuations, balances with phase-sensing error in interferometric gravity-wave detectors to prevent position-measurement accuracy from surpassing the SQL. In Sec. V we first show that this balance occurs in single-frequency interferometers because of the energy-phase uncertainty principle. Next, making use of recent work on phase and amplitude uncertainties in heterodyne detec-

tion,<sup>3</sup> we show that the energy-phase uncertainty principle can be circumvented in a two-frequency squeezed-state interferometer. Here we find that position-sensing accuracy far better than the SQL is predicted at photon numbers substantially larger than those for a coherent-state single-frequency interferometer running at the SQL. This performance analysis complements the work of Yuen,<sup>4</sup> who has questioned the validity of the SQL on fundamental grounds. Our analysis assumes that ideal photodetectors respond to photon flux rather than energy flux. This question is not yet fully resolved.

## II. SQUEEZED STATES, DIRECT AND HOMODYNE DETECTION

The properties of squeezed states, also called two-photon coherent states, have been treated extensively by Yuen.<sup>5</sup> Using his notation, the single-mode squeezed state  $|\beta; \mu, \nu\rangle$  is parametrized by three complex numbers  $\beta$ ,  $\mu$ , and  $\nu$  with  $|\mu|^2 - |\nu|^2 = 1$ . If  $a$  denotes the photon annihilation operator for the electromagnetic field mode in question, then the state  $|\beta; \mu, \nu\rangle$  is defined to be the eigenstate of the operator

$$b = \mu a + \nu a^\dagger \quad (1)$$

with eigenvalue  $\beta$ .

The statistics of direct, homodyne, and heterodyne detection of multimode quantized fields are conveniently calculated from the results of Yuen and Shapiro.<sup>6</sup> Direct detection, with a unity quantum efficiency detector, of the single mode with annihilation operator  $a$  measures the photon-number operator  $N = a^\dagger a$ . When the state of the mode is  $|\beta; \mu, \nu\rangle$  the  $N$  measurement has the mean value

$$\langle N \rangle = |\hat{\beta}|^2 + |\nu|^2 \quad (2)$$

and variance

$$\langle \Delta N^2 \rangle = |\mu \hat{\beta} - \nu \hat{\beta}^*|^2 + 2|\mu \nu|^2, \quad (3)$$

where

$$\langle a \rangle = \mu^* \beta - \nu \beta^* \equiv \hat{\beta}. \quad (4)$$

For  $\beta, \mu, \nu$  positive real valued, Eq. (3) reduces to

$$\begin{aligned} \langle \Delta N^2 \rangle &= (\langle N \rangle - \nu^2)[(1 + \nu^2)^{1/2} - \nu]^2 + 2\nu^2(1 + \nu^2) \\ &\approx (\langle N \rangle - \nu^2)/4\nu^2 + 2\nu^2(1 + \nu^2), \end{aligned} \quad (5)$$

where the approximation is valid for  $\langle N \rangle \geq \nu^2 \gg 1$ . Minimizing the right member of (5) with respect to  $\nu^2$  at constant  $\langle N \rangle$  yields

$$\langle \Delta N^2 \rangle_{\min} \approx \langle N \rangle^{2/3} \quad (6)$$

at

$$\langle N \rangle = 16\nu^6 \gg 1. \quad (7)$$

Thus, the maximum direct-detection SNR one may achieve using a single-mode squeezed state is

$$\begin{aligned} \text{SNR}_{\max} &= \langle N \rangle^2 / \langle \Delta N^2 \rangle_{\min} \\ &= \langle N \rangle^{4/3}, \text{ for } \langle N \rangle \gg 1, \end{aligned} \quad (8)$$

which is far superior to the coherent-state (CS) result

$$\text{SNR}_{\text{CS}} = \langle N \rangle \quad (9)$$

for direct detection at the same average photon number.

Optical homodyne detection, with a unity quantum efficiency detector, of the single mode with annihilation operator  $a$  measures the field quadrature operator  $(ae^{j\psi} + a^\dagger e^{-j\psi})/2$ , where  $\psi$  is the phase difference between the mode being measured and the local-oscillator field. When  $\psi=0$  and the state of the  $a$  mode is  $|\beta; \mu, \nu\rangle$ , this becomes a measurement of

$$a_1 = (a + a^\dagger)/2, \quad (10)$$

with mean value

$$\langle a_1 \rangle = \text{Re}(\hat{\beta}) \quad (11)$$

and variance

$$\langle \Delta a_1^2 \rangle = |\mu - \nu|^2 / 4. \quad (12)$$

For a fixed average photon number  $\langle N \rangle$ , Eqs. (11) and (12) imply the following maximum homodyne-detection signal-to-noise ratio:<sup>2</sup>

$$\begin{aligned} \text{SNR}_{\max} &= (\langle a_1 \rangle^2 / \langle \Delta a_1^2 \rangle)_{\max} \\ &= 4\langle N \rangle(\langle N \rangle + 1), \end{aligned} \quad (13)$$

which is achieved with  $\beta, \mu, \nu$  real valued and

$$\mu = (\langle N \rangle + 1) / (2\langle N \rangle + 1)^{1/2}, \quad (14)$$

$$\nu = \langle N \rangle / (2\langle N \rangle + 1)^{1/2}. \quad (15)$$

When  $\langle N \rangle \gg 1$ , (13) represents a significant improvement over both the optimized coherent-state homodyne detection performance

$$\text{SNR}_{\text{CS}} = 4\langle N \rangle, \quad (16)$$

and the optimized squeezed-state direct detection performance (8).

Physically, the preceding  $\text{SNR}_{\max}$  advantage of homodyne detection over direct detection can be justified. The squeezed state  $|\beta; \mu, \nu\rangle$  with  $\mu, \nu$  positive real valued, is a minimum-uncertainty state for the Heisenberg inequality

$$\langle \Delta a_1^2 \rangle \langle \Delta a_2^2 \rangle \geq \frac{1}{16}, \quad (17)$$

where  $a_2 = (a - a^\dagger)/2j$  is the conjugate observable to  $a_1$  and

$$\begin{aligned} \langle \Delta a_1^2 \rangle &= [(1 + \nu^2)^{1/2} - \nu]^2 / 4 \\ &\approx 1/16\nu^2, \text{ for } \nu^2 \gg 1. \end{aligned} \quad (18)$$

The right member of (18) is far superior to the coherent-state value  $\langle \Delta a_1^2 \rangle_{\text{CS}} = \frac{1}{4}$ , hence the advantage of (13) over (16). On the other hand, for the photon-number operator we have

$$N = a^\dagger a = a_1^2 + a_2^2 - \frac{1}{2}. \quad (19)$$

Thus, direct detection of the squeezed state  $|\beta; \mu, \nu\rangle$  with  $\mu, \nu$  positive real valued is sensitive to both the low-noise quadrature component (18), and the high-noise quadrature component

$$\begin{aligned} \langle \Delta a_2^2 \rangle &= [(1+\nu^2)^{1/2} + \nu]^2 / 4 \\ &\approx \nu^2, \text{ for } \nu^2 \gg 1, \end{aligned} \quad (20)$$

hence the advantage of (13) over (8).

### III. SINGLE-FREQUENCY INTERFEROMETER ANALYSIS

Figure 1 shows an archetypal single-frequency interferometer whose behavior we shall analyze quantum mechanically. The boxes  $e^{j\theta}$  and  $e^{j\phi}$  represent the excess phase shifts (beyond some reference value) incurred by the monochromatic light beams as they propagate through the signal and reference arms of the system, respectively. The annihilation operators,  $a^{\text{out}}$  and  $b^{\text{out}}$ , for the single-mode output fields are related to the relevant single-mode input-field annihilation operators,  $a^{\text{in}}$  and  $b^{\text{in}}$ , via the unitary transformation

$$\begin{bmatrix} a^{\text{out}} \\ b^{\text{out}} \end{bmatrix} = e^{j\Phi} \begin{bmatrix} j \sin(\delta) & \cos(\delta) \\ \cos(\delta) & j \sin(\delta) \end{bmatrix} \begin{bmatrix} a^{\text{in}} \\ b^{\text{in}} \end{bmatrix}, \quad (21)$$

where

$$\Phi = (\theta + \phi) / 2, \quad (22)$$

and

$$\delta = (\theta - \phi) / 2. \quad (23)$$

A knowledge of the states of the  $a^{\text{in}}$  and  $b^{\text{in}}$  modes in conjunction with the transformation (21) is sufficient to completely characterize the quantum states of the output modes.

It should be noted that although Fig. 1 is in the form of a Mach-Zehnder (MZ) interferometer, the unitary transformation (21) also applies to a Michelson interferometer. In either case, information concerning the signal arm phase shift  $\theta$  may be extracted from either  $\Phi$  or  $\delta$ , depending on the optical detection scheme employed. We should also note that the temporal coherence that is implicit in our single-frequency formulation permits us to dispense with the input beamsplitter, and consider the modes associated with the annihilation operators  $\tilde{a}$  and  $\tilde{b}$  of Fig. 1 to be the inputs. This approach will be of use in Sec. V. Our interest in the present section is to determine the best operating point for a homodyne-detection squeezed-state interferometer.

Without significant loss of generality, we shall assume that the  $a^{\text{in}}$  and  $b^{\text{in}}$  modes are in the minimum-uncertainty squeezed states  $|\beta_1; \mu_1, \nu_1\rangle$  and  $|\beta_2; \mu_2, \nu_2\rangle$ , respectively, where  $\{\mu_i, \nu_i; i=1,2\}$  are real valued. We shall also assume that homodyne detection is used to measure  $a_1^{\text{out}} = (a^{\text{out}} + a^{\text{out}\dagger})/2$ , and we will use  $y$  to denote the classical random-variable outcome of this measurement. We want to choose the interferometer's operating point, i.e., the state parameters  $\{\beta_i, \mu_i, \nu_i\}$  and the reference-arm phase shift  $\phi$ , to optimize the estimate of the signal-arm phase shift  $\theta$  that can be obtained from the data  $y$ . This optimization involves three performance criteria: (1) the average measurement outcome  $\langle y \rangle$  should be a linear function of  $\theta$  for  $|\theta| \ll 1$ ; (2) the variance of the measurement outcome  $\langle \Delta y^2 \rangle$  should be minimized at con-

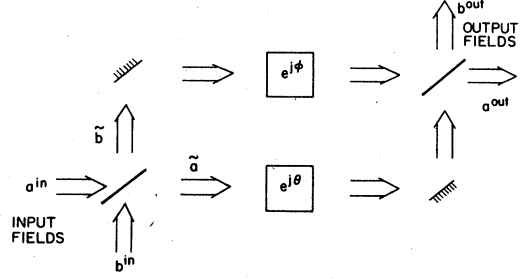


FIG. 1. Basic interferometric precision-measurement device.

stant  $\langle y \rangle$ ; and (3) the measurement noise should not depend on the signal phase shift, i.e.,  $\langle \Delta y^2 \rangle$  should be  $\theta$  independent. The first criterion permits straightforward linear data processing to be employed. The second criterion amounts to seeking a maximum SNR operating point. The third criterion is a subtlety whose importance will be made clear later.

In pursuing the foregoing optimization, the method of antinormally ordered characteristic functions<sup>5,7</sup> is particularly germane. A single-mode field with annihilation operator  $a$  in a state described by a density operator  $\rho$  has antinormally ordered characteristic function

$$\begin{aligned} \chi_A(\underline{\eta}_q) &= \text{tr} \{ \rho \exp [ -(\eta_1 a_1 + \eta_2 a_2) - j(\eta_1 a_2 - \eta_2 a_1) ] \\ &\quad \times \exp [ (\eta_1 a_1 + \eta_2 a_2) - j(\eta_1 a_2 - \eta_2 a_1) ] \}, \end{aligned} \quad (24)$$

where

$$\underline{\eta}_q = \begin{bmatrix} 2\eta_2 \\ -2\eta_1 \end{bmatrix}, \text{ with } \eta_1, \eta_2 \text{ real valued}, \quad (25)$$

and  $a_1$  and  $a_2$  are the quadrature components of  $a$  [see Eqs. (10), (17)]. For the squeezed state  $|\beta; \mu, \nu\rangle$  we have<sup>5</sup>

$$\chi_A(\underline{\eta}_q) = \exp [ j \underline{\eta}_q^T \underline{\alpha}_q - 2^{-1} \underline{\eta}_q^T (\Lambda_s + I/4) \underline{\eta}_q ], \quad (26)$$

where

$$\underline{\alpha}_q = \begin{bmatrix} (\hat{\beta} + \hat{\beta}^*) / 2 \\ (\hat{\beta} - \hat{\beta}^*) / 2j \end{bmatrix}, \quad (27)$$

$$\Lambda_s = 4^{-1} \begin{bmatrix} |\mu - \nu|^2 & 2 \text{Im}(\mu \nu^*) \\ 2 \text{Im}(\mu \nu^*) & |\mu + \nu|^2 \end{bmatrix}, \quad (28)$$

$T$  denotes transpose, and  $I$  is the  $2 \times 2$  identity matrix. Equation (26) is especially convenient for our purposes, in that homodyne detection of  $a_1$  for a mode whose characteristic function takes this form yields a classical outcome  $y$  that is Gaussian distributed with  $\langle y \rangle = \underline{e}_1^T \underline{\alpha}_q$  and  $\langle \Delta y^2 \rangle = \underline{e}_1^T \Lambda_s \underline{e}_1$ , where  $\underline{e}_1^T = [1, 0]$ .

From (21), (24) and the assumed input states to the interferometer it is now straightforward to show that the characteristic function for the density operator of the  $a^{\text{out}}$  mode is given by (26) with

$$\underline{\alpha}_q = 2^{-1} \begin{bmatrix} \text{Re}[(e^{j\theta} - e^{j\phi})\hat{\beta}_1 + (e^{j\theta} + e^{j\phi})\hat{\beta}_2] \\ \text{Im}[(e^{j\theta} - e^{j\phi})\hat{\beta}_1 + (e^{j\theta} + e^{j\phi})\hat{\beta}_2] \end{bmatrix}, \quad (29)$$

and

$$\underline{e}_1^T \Lambda_s \underline{e}_1 = c_{12}(\cos\theta + \cos\phi)^2 + c_{22}(\sin\theta + \sin\phi)^2 + c_{11}(\cos\theta - \cos\phi)^2 + c_{21}(\sin\theta - \sin\phi)^2, \quad (30a)$$

$$\underline{e}_1^T \Lambda_s \underline{e}_2 = \underline{e}_2^T \Lambda_s \underline{e}_1 = -(c_{21} - c_{11} + c_{22} - c_{12})(\sin 2\theta + \sin 2\phi)/2 + (c_{21} - c_{11} - c_{22} + c_{12})\sin(\theta + \phi), \quad (30b)$$

$$\underline{e}_2^T \Lambda_s \underline{e}_2 = c_{22}(\cos\theta + \cos\phi)^2 + c_{12}(\sin\theta + \sin\phi)^2 + c_{11}(\sin\theta - \sin\phi)^2 + c_{21}(\cos\theta - \cos\phi)^2, \quad (30c)$$

where

$$\underline{e}_2^T = [0, 1], \quad (31)$$

$$\hat{\beta}_i = \mu_i \beta_i - \nu_i \beta_i^*, \quad \text{for } i = 1, 2,$$

and

$$c_{ij} = \{[\mu_j + (-1)^i \nu_j]/4\}^2, \quad \text{for } i, j = 1, 2. \quad (32)$$

As an illustration of the use of Eqs. (26) and (29)–(32), let us consider the MZ interferometer. We shall assume that the excess phase shifts  $\theta$  and  $\phi$  obey  $|\theta| \ll 1$ ,  $\phi = 0$ , i.e., the signal arm incurs a very small shift from the reference-arm phase. We have that our homodyne observation of  $a_1^{\text{out}}$  yields a Gaussian random variable  $y$  with mean value

$$\langle y \rangle = \text{Re}[j\theta(\hat{\beta}_1 + \hat{\beta}_2) + 2\hat{\beta}_2]/2 \quad (33)$$

to lowest order in  $\theta$ . We can enforce our first performance criterion, namely, making  $\langle y \rangle \propto \theta$  for  $|\theta| \ll 1$ , by choosing  $\beta_2 = -j\beta$  for  $\beta$  real and  $\beta_1 = 0$  so that Eqs. (31) and (33) yield

$$\langle y \rangle = \theta(\mu_2 + \nu_2)\beta/2. \quad (34)$$

To maximize the strength of the mean we will take  $\mu_2 = \mu > 0$  and  $\nu_2 = \nu > 0$ , hence determining the state of the  $b^{\text{in}}$  mode to be  $|-j\beta; \mu, \nu\rangle$ . Turning to the variance of  $y$  we find

$$\langle \Delta y^2 \rangle = (\mu - \nu)^2/4 + \theta^2[4\mu\nu + (\mu_1 + \nu_1)^2 - (\mu - \nu)^2]/16 \quad (35)$$

to second order in  $\theta$ . We shall assume  $\mu_1 = \mu, \nu_1 = -\nu$  (making the state of the  $a^{\text{in}}$  mode  $|0; \mu, -\nu\rangle$ ) to reduce (35) to

$$\langle \Delta y^2 \rangle = (\mu - \nu)^2/4 + \theta^2\mu\nu/4. \quad (36)$$

We now have the following results. The estimate of  $\theta$  based on  $y$

$$\hat{\theta} = 2y/\beta(\mu + \nu) \quad (37)$$

is unbiased

$$\langle \hat{\theta} \rangle = \theta \quad (38)$$

with a mean-square error

$$\xi = \langle (\hat{\theta} - \theta)^2 \rangle = (\mu - \nu)^2/\beta^2(\mu + \nu)^2 \quad (39)$$

when  $|\theta| \ll 1$ . Using the fact that

$$N_T \equiv \langle a^{\text{in}\dagger} a^{\text{in}} \rangle + \langle b^{\text{in}\dagger} b^{\text{in}} \rangle = \beta^2(\mu + \nu)^2 + 2\nu^2 \quad (40)$$

is the average number of photons entering the interferometer, it is easily shown that

$$\xi \approx 1/4\nu^2(N_T - 2\nu^2) \quad (41)$$

for  $\nu^2 \gg 1$ . Equation (41) can be minimized with respect to  $\nu^2$  at fixed  $N_T$  to give

$$\xi_{\text{min}} = 2/N_T^2, \quad \text{for } N_T \gg 1, \quad (42)$$

as compared to the coherent-state performance

$$\xi_{\text{CS}} = 1/N_T. \quad (43)$$

Although we have not been particularly careful to show that our  $\{\mu_i, \nu_i\}$  choices are the best, it can be demonstrated that  $\xi_{\text{min}} \propto N_T^{-2}$  is the optimum mean-square error behavior of the homodyne-detection squeezed-state MZ interferometer. At this juncture, however, we can point out the significance of our third performance criterion. For the MZ interferometer with a mean-square error given by (42) we cannot measure  $\theta$  accurately for  $|\theta| \leq 2^{1/2}/N_T \equiv \theta_{\text{min}}$ . Assuming that  $|\theta| = \theta_{\text{min}}$ , we find that the  $\theta^2$  term on the right-hand side in (36) is of the same order of magnitude as the zeroth-order term in this expression. The analysis leading from (36) to (42) assumed this  $\theta^2$  term to be negligible, but such is not the case for  $|\theta| \geq \theta_{\text{min}}$ . This  $\theta$  dependence of  $\langle \Delta y^2 \rangle$  comes about because the state of the  $a^{\text{out}}$  mode (or for that matter the  $b^{\text{out}}$  mode) is not a minimum-uncertainty squeezed state when the MZ interferometer input modes are  $|0; \mu, -\nu\rangle$  and  $|-j\beta; \mu, \nu\rangle$  and  $\theta \neq 0, \nu \neq 0$ .

The problem of  $\theta$  dependence in  $\langle \Delta y^2 \rangle$  recurs if we pursue a similar analysis for the Michelson interferometer. To truly optimize interferometer design, we want a system whose output states will be minimum-uncertainty squeezed states when its input states are minimum-uncertainty squeezed states. This property is held by what we call phase-conjugate interferometers, i.e., systems for which the reference-arm phase shift equals the conjugate of the signal-arm phase shift ( $\phi = -\theta$ ). With input states  $|-j\beta; \mu, -\nu\rangle$  and  $|0; \mu, \nu\rangle$  for the  $a^{\text{in}}$  and  $b^{\text{in}}$  modes, respectively, (30) reduces to

$$\Lambda_s = \text{diag}[(\mu - \nu)^2/4, (\mu + \nu)^2/4], \quad (44)$$

for the phase-conjugate interferometer regardless of the value of  $\theta$ . Moreover, (29) yields

$$\langle y \rangle = \theta(\mu - \nu)\beta, \quad \text{for } |\theta| \ll 1, \quad (45)$$

from which it can be shown that

$$\hat{\theta} = y/\beta(\mu - \nu) \quad (46)$$

is unbiased with mean-square error

$$\xi = 1/4\beta^2 = (\mu - \nu)^2/4(N_T - 2\nu^2), \quad (47)$$

where  $N_T$  is the average number of photons entering the interferometer. Equation (47) leads us to  $\xi_{\text{min}} = 1/2N_T^2$ , essentially the same as that found for the MZ system, only here there is no unwarranted assumption of neglecting  $\theta$  dependence in  $\langle \Delta y^2 \rangle$ .

#### IV. SINGLE-FREQUENCY INTERFEROMETRIC GRAVITY-WAVE DETECTION

Figure 2 shows a single-frequency phase-conjugate interferometer for gravity-wave detection. As a gravity wave displaces the mass  $M$ , the phase shift in one arm of the system increases while the phase shift in the other arm decreases by the same amount. The light in each arm of the interferometer makes  $b$  round trips between its end mirror and the mass  $M$  before exiting the system, and so the time spent within each arm is

$$\tau = 2bl/c, \quad (48)$$

where  $c$  is the speed of light. To apply the analysis of Sec. III to Fig. 2 we identify  $\theta$  as  $2b\delta l\omega/c$ , where  $\delta l$  is the differential displacement of  $M$  induced by the gravity wave, and  $\omega$  is the radian frequency of the light. We want to estimate  $\delta l$  in the regime  $|2b\delta l\omega/c| \ll 1$  using squeezed states and homodyne detection of  $a_1^{\text{out}}$ , and compare the resulting performance with that obtained by Caves<sup>1</sup> for squeezed states and direct detection.

According to Caves, there are three sources of error that limit our ability to measure  $\delta l$ . The first is the intrinsic quantum-mechanical uncertainty, called the standard quantum limit (SQL), in determining the position of a free mass that arises from the  $\Delta p \Delta q \geq \hbar/2$  Heisenberg inequality; Caves *et al.*<sup>8</sup> have shown the SQL restricts  $\delta l$  measurement accuracy to about  $\pm(\hbar\tau/M)^{1/2}$ . The second source of error is just the noise associated with the detection process, and the third source of error is the so-called back action of the interferometer in the form of radiation pressure fluctuations on the mirrors attached to  $M$ . According to Caves,<sup>1</sup> the intrinsic uncertainty need not be considered explicitly, because it represents a lower limit which may be approached, but never surpassed, with proper control of the other error sources. Furthermore, the detection and radiation-pressure errors, when properly balanced, must enforce the SQL.<sup>1,9</sup>

Following the preceding error-analysis prescription we assume that the total mean-square error,  $\xi$ , in the position estimate  $\delta \hat{l}$  can be decomposed into detection noise and radiation pressure components, viz.,

$$\xi = \xi_{\text{det}} + \xi_{\text{rp}}. \quad (49)$$

For homodyne detection of  $a_1^{\text{out}}$  in Fig. 2, with input states  $|-j\beta; \mu, -\nu\rangle$  and  $|0; \mu, \nu\rangle$  for  $a^{\text{in}}$  and  $b^{\text{in}}$ , respectively, and  $\delta \hat{l} = c\hat{\theta}/2b\omega$  with  $\hat{\theta}$  from (46), we have that

$$\xi_{\text{det}} = (c/8b\omega\hat{\beta}\nu)^2, \quad \text{for } \nu \gg 1, \quad (50)$$

where  $\hat{\beta} = \beta(\mu - \nu)$ . The error due to radiation pressure fluctuations is proportional to the difference in the number of photons impinging on the two sides of  $M$ . Defining a differential momentum-transfer operator

$$\Delta p = 2b\hbar\omega(\hat{a}^\dagger\hat{a} - \hat{b}^\dagger\hat{b})/c, \quad (51)$$

we find that  $\langle \Delta p \rangle = 0$  and

$$\xi_{\text{rp}} = (\tau/M)^2 \langle \Delta p^2 \rangle = (4b\hbar\tau\omega\nu\hat{\beta}/Mc)^2. \quad (52)$$

Combining (49), (50), and (52), and minimizing  $\xi$  with respect to  $\nu^2$  and  $\hat{\beta}^2$ , we obtain

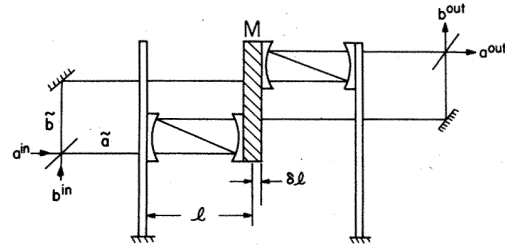


FIG. 2. Phase-conjugate interferometer for gravity-wave detection.

$$\xi_{\text{min}} = \hbar\tau/M \equiv \text{SQL}. \quad (53)$$

The minimum average number of input photons required to achieve this performance turns out to be

$$N_{T\text{min}} = N_{\text{CS}}^{1/2}, \quad (54)$$

where

$$N_{\text{CS}} = Mc^2/8\hbar\omega^2b^2\tau \quad (55)$$

is the average photon number required to run a coherent-state interferometer at the SQL. Because  $N_{\text{CS}} \gg 1$  for realistic interferometer parameters, (54) is a substantial improvement over (55).

The preceding single-frequency homodyne analysis is consistent with Caves's view that detection noise plus radiation-pressure back action enforce the SQL; the use of squeezed states permits a reduction in the photon number needed to reach, but not surpass, the SQL. Based on Sec. II, one should expect (54) to be lower than the photon-number requirement for a direct-detection squeezed-state interferometer to reach the SQL. However, Caves's analysis<sup>1</sup> of differenced direct detection (analogous to measuring  $a^{\text{out}\dagger}a^{\text{out}} - b^{\text{out}\dagger}b^{\text{out}}$  in Fig. 2) in a squeezed-state interferometer for gravity-wave detection shows SQL performance being reached (with a different operating point than ours) at the same  $N_{T\text{min}}$  given by (54). It turns out there is no contradiction between Sec. II and the equivalence of optimized differenced direct-detection and homodyne-detection squeezed-state interferometers. The use of differenced direct-detection was not explicitly treated in Sec. II. Such an arrangement can favorably exploit nonclassical photocounting correlations that exist between the states of the  $a^{\text{out}}$  and  $b^{\text{out}}$  modes. In particular,<sup>10</sup> for a classical output state, i.e., when the density operator for the states of the output modes has a joint  $P$  representation with a non-negative  $P$  function, we have the semiclassical lower bound

$$\langle \Delta(a^{\text{out}\dagger}a^{\text{out}} - b^{\text{out}\dagger}b^{\text{out}})^2 \rangle \geq \langle a^{\text{out}\dagger}a^{\text{out}} \rangle + \langle b^{\text{out}\dagger}b^{\text{out}} \rangle, \quad (56)$$

whereas for a nonclassical output state, e.g., a squeezed state, we have the quantum-mechanical lower bound

$$\langle \Delta(a^{\text{out}\dagger}a^{\text{out}} - b^{\text{out}\dagger}b^{\text{out}})^2 \rangle \geq 0. \quad (57)$$

Note that no such nonclassical correlations are available for homodyne detection, hence processing both  $a^{\text{out}}$  and  $b^{\text{out}}$  in the homodyne-detection interferometer offers no significant gain in performance. On the other hand,

Caves's differenced direct-detection interferometer<sup>1</sup> is not a phase-conjugate system, and so it suffers from  $\delta l$  dependence in its detection noise. Indeed, just as was noted following (43), certain variance terms which Caves discards turn out to be larger, although of the same magnitude, as the terms he retains. This  $\delta l$  dependence of the detection noise may not be of practical concern, but from a theoretical standpoint it makes it unlikely that the differenced direct-detection system could truly achieve the SQL.

### V. BEYOND THE STANDARD QUANTUM LIMIT

In recent work, Yuen<sup>4</sup> has cast doubt on the usual derivation<sup>8</sup> of the SQL from the  $\Delta p \Delta q$  uncertainty principle. Yuen argues that the standard approach neglects correlations that may exist between  $p$  and  $q$ . Moreover, he has shown that there is a general class of free-particle states, which he calls twisted coherent states, for which the accuracy of a position measurement is not constrained by the SQL. In this section we shall develop a complementary result, namely, a conceptual design for a gravity-wave detecting interferometer whose performance surpasses the SQL. The principal price paid in our design is that single-frequency fields can no longer be used.

For the interferometer shown in Fig. 2, the mean-square estimation error can be written in the form

$$\xi = \text{SQL}(\langle \Delta N^2 \rangle / N_{\text{CS}} + N_{\text{CS}} \langle \Delta \Phi^2 \rangle), \quad (58)$$

where the first term represents the radiation pressure error contribution in terms of an appropriate photon number variance, and the second term represents the detection error contribution in terms of an appropriate phase variance. This expression applies for arbitrary quantum states. Because the cases considered thus far were all sin-

gle frequency, the phase-energy uncertainty principle<sup>11,12</sup> can be used to show

$$\xi \geq \text{SQL} \{ 1/4 N_{\text{CS}} \langle \Delta \Phi^2 \rangle + N_{\text{CS}} \langle \Delta \Phi^2 \rangle \}, \quad (59)$$

which has a minimum equal to the SQL. Thus, in our view, it is not the radiation-pressure back action *per se* that prevents the single-frequency interferometer from outperforming the SQL, rather it is the fact that the radiation-pressure error is inextricably tied to the detection error through  $\langle \Delta N^2 \rangle \langle \Delta \Phi^2 \rangle \geq \frac{1}{4}$ . Furthermore, the exact prescription we shall need to circumvent this uncertainty principle has recently been developed by Shapiro and Wagner.<sup>3</sup> They have analyzed the quantum limits on squared-amplitude ( $U$ ) and phase ( $\Phi$ ) measurements made via optical heterodyne detection,<sup>13</sup> and shown that a particular multimode two-photon coherent state (squeezed state<sup>14</sup>) permits  $\langle \Delta U^2 \rangle \rightarrow 0$  and  $\langle \Delta \Phi^2 \rangle \rightarrow 0$  to be achieved simultaneously.

Consider the two-frequency interferometer shown in Fig. 3, where we have dispensed with the input beam-splitter from the Fig. 2 configuration and replaced  $\tilde{a}$  and  $\tilde{b}$  with dual-mode field operators

$$E_a(t) = a_+ \exp[-j(\omega + \omega_{\text{IF}})t] + a_- \exp[-j(\omega - \omega_{\text{IF}})t] \quad (60)$$

and

$$E_b(t) = b_+ \exp[-j(\omega + \omega_{\text{IF}})t] + b_- \exp[-j(\omega - \omega_{\text{IF}})t], \quad (61)$$

where we have suppressed space and time normalization constants,  $\omega$  is an optical frequency,  $\omega_{\text{IF}}$  is a radio (intermediate) frequency, and  $\{a_+, a_-, b_+, b_-\}$  are a canonical

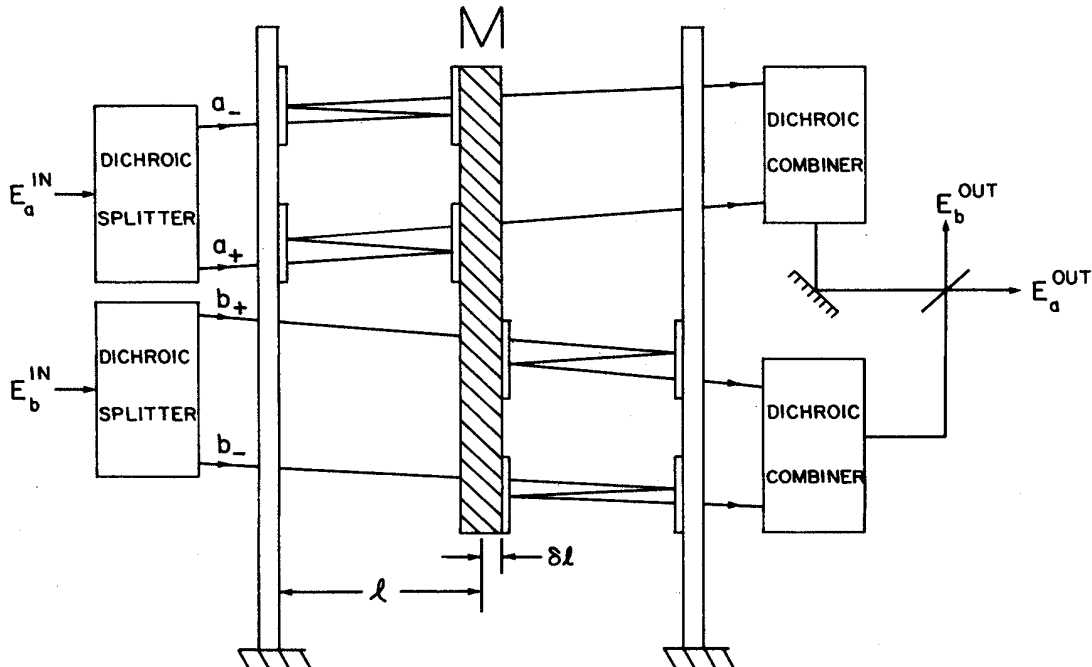


FIG. 3. Two-frequency interferometer for gravity-wave detection.

set of photon annihilation operators. These fields are split into their constituent frequency components by the action of lossless passive grating/mirror arrangements that are labeled dichroic splitters in Fig. 3. The four separate field

$$E_a^{\text{out}}(t) = 2^{-1/2} e^{-j\omega t} \{ a_+ \exp[j(\omega + \omega_{\text{IF}})2b\delta l/c \cos(\theta_+)] + b_+ \exp[-j(\omega + \omega_{\text{IF}})2b\delta l/c \cos(\theta_+)] \} e^{-j\omega_{\text{IF}}t} \\ + \{ a_- \exp[j(\omega - \omega_{\text{IF}})2b\delta l/c \cos(\theta_-)] + b_- \exp[-j(\omega - \omega_{\text{IF}})2b\delta l/c \cos(\theta_-)] \} e^{j\omega_{\text{IF}}t} \quad (62)$$

and

$$E_b^{\text{out}}(t) = 2^{-1/2} e^{-j\omega t} \{ a_+ \exp[j(\omega + \omega_{\text{IF}})2b\delta l/c \cos(\theta_+)] - b_+ \exp[-j(\omega + \omega_{\text{IF}})2b\delta l/c \cos(\theta_+)] \} e^{-j\omega_{\text{IF}}t} \\ + \{ a_- \exp[j(\omega - \omega_{\text{IF}})2b\delta l/c \cos(\theta_-)] - b_- \exp[-j(\omega - \omega_{\text{IF}})2b\delta l/c \cos(\theta_-)] \} e^{j\omega_{\text{IF}}t} \quad (63)$$

are obtained from the final beamsplitter, where we have assumed that  $2b(\omega + \omega_{\text{IF}})l/c \cos(\theta_+)$  and  $2b(\omega - \omega_{\text{IF}})l/c \cos(\theta_-)$  are both integral multiples of  $2\pi$ .

If we heterodyne detect  $E_a^{\text{out}}(t)$  and  $E_b^{\text{out}}(t)$  with local-oscillator lasers of frequency  $\omega$ , then synchronously demodulate the cosine quadrature of the  $E_a^{\text{out}}$  intermediate-frequency signal and the sine quadrature of the  $E_b^{\text{out}}$  intermediate-frequency signal and add the results, we obtain a real-valued classical random variable  $y$  whose statistics coincide with those of the operator measurement<sup>3,6,13</sup>

$$\tau^{-1} \int \{ \text{Re}[E_a^{\text{out}}(t)e^{j\omega t}] \cos(\omega_{\text{IF}}t) + \text{Re}[E_b^{\text{out}}(t)e^{j\omega t}] \sin(\omega_{\text{IF}}t) \} dt \\ = 2^{-3/2} \{ (a_{+1} + b_{+1} + a_{-1} + b_{-1} + a_{+2} - b_{+2} - a_{-2} + b_{-2}) \\ - (2b\delta l/c) [(\omega + \omega_{\text{IF}})(a_{+2} - b_{+2} - a_{-1} - b_{-1})/\cos(\theta_+) + (\omega - \omega_{\text{IF}})(a_{-2} - b_{-2} + a_{-1} + b_{-1})/\cos(\theta_-)] \} \quad (64)$$

Here, the integration is over an appropriate  $\tau$ -sec interval,  $|2b(\omega + \omega_{\text{IF}})\delta l/c \cos(\theta_+)| \ll 1$  and  $|2b(\omega - \omega_{\text{IF}})\delta l/c \cos(\theta_-)| \ll 1$  are assumed, and we have used our usual notation for the quadrature components of an annihilation operator. Next we introduce another canonical set of photon annihilation operators via the transformations<sup>3</sup>

$$\begin{bmatrix} c_+ \\ c_- \end{bmatrix} = 2^{-1/2} \begin{bmatrix} 1 & 1 \\ 1 & -1 \end{bmatrix} \begin{bmatrix} a_+^{\text{in}} \\ a_-^{\text{in}} \end{bmatrix} \quad (65)$$

and

$$\begin{bmatrix} d_+ \\ d_- \end{bmatrix} = 2^{-1/2} \begin{bmatrix} 1 & 1 \\ 1 & -1 \end{bmatrix} \begin{bmatrix} b_+^{\text{in}} \\ b_-^{\text{in}} \end{bmatrix} \quad (66)$$

in terms of which the right member of (64) becomes

$$2^{-1} [(c_{+1} + d_{+1})(1 + A) - (c_{+2} - d_{+2} - c_{-1} - d_{-1})B \\ + (c_{-2} - d_{-2})(1 - A)],$$

where, because of radiation-pressure error considerations (see below), we have chosen  $\theta_+$  and  $\theta_-$  to force

$$\bar{\omega} = (\omega + \omega_{\text{IF}})\cos(\theta_+) = (\omega - \omega_{\text{IF}})\cos(\theta_-) \quad (67)$$

for a frequency  $\bar{\omega}$  slightly below  $\omega - \omega_{\text{IF}}$ , and

$$A \equiv 8\omega\omega_{\text{IF}}b\delta l/c\bar{\omega}, \quad (68a)$$

$$B \equiv 4(\omega^2 + \omega_{\text{IF}}^2)b\delta l/c\bar{\omega}. \quad (68b)$$

We shall assume that the modes associated with the annihilation operators  $c_+$ ,  $d_+$ ,  $c_-$ , and  $d_-$  are placed in the independent squeezed states  $|\beta; \mu, \nu\rangle$ ,  $|\beta; \mu, \nu\rangle$ ,  $|-j\beta; \mu, -\nu\rangle$ , and  $|j\beta; \mu, -\nu\rangle$ , respectively, where  $\beta, \mu, \nu$

now enter plane-parallel mirror systems at small angles  $\theta_+$  and  $\theta_-$  to the  $\delta l$  axis for modes with frequencies  $\omega + \omega_{\text{IF}}$  and  $\omega - \omega_{\text{IF}}$ , respectively. After dichroic beam combination, output fields

are positive real. It can then be shown that  $y$  is a Gaussian random variable with a mean value of

$$\langle y \rangle = (16b\hat{\beta}\omega\omega_{\text{IF}}/c\bar{\omega})\delta l \quad (69)$$

and variance

$$\langle \Delta y^2 \rangle = (\mu - \nu)^2/4 + B^2(\mu + \nu)^2/4, \quad (70)$$

where  $\hat{\beta} \equiv \beta(\mu - \nu)$ . We shall assume that the second term on the right-hand side in (70) is negligible. Physically, the high-noise quadrature contribution arises because our two-frequency system is not exactly phase conjugate in the sense of Sec. III. We shall check later that the preceding assumption is valid.

Based on (69) and  $\langle \Delta y^2 \rangle = (\mu - \nu)^2/4$  we have that

$$\hat{\delta l} = y / (16b\hat{\beta}\omega\omega_{\text{IF}}/c\bar{\omega}) \quad (71)$$

is an unbiased estimate of  $\delta l$  with mean-square detection error

$$\xi_{\text{det}} = (\mu - \nu)^2 / (32b\hat{\beta}\omega\omega_{\text{IF}}/c\bar{\omega})^2 \\ \approx (c\bar{\omega}/32b\omega\omega_{\text{IF}})^2 / 4\hat{\beta}^2\nu^2 \text{ for } \nu \gg 1. \quad (72)$$

The radiation-pressure contribution to the mean-square position error is computed as follows. The differential momentum-transfer operator for the  $\delta l$  axis is

$$\Delta p = 2b\hbar [(\omega + \omega_{\text{IF}})(a_+^\dagger a_+ - b_+^\dagger b_+)\cos(\theta_+) \\ + (\omega - \omega_{\text{IF}})(a_-^\dagger a_- - b_-^\dagger b_-)\cos(\theta_-)]/c \\ = (2b\hbar\bar{\omega}/c)(a_+^\dagger a_+ + a_-^\dagger a_- - b_+^\dagger b_+ - b_-^\dagger b_-). \quad (73)$$

It follows that [see (52)]

$$\begin{aligned}
\xi_{rp} &= (2b\hbar\bar{\omega}\tau/Mc)^2 \langle [\Delta(a_+^\dagger a_+ + a_-^\dagger a_- - b_+^\dagger b_+ - b_-^\dagger b_-)]^2 \rangle \\
&= (2b\hbar\bar{\omega}\tau/Mc)^2 \langle [\Delta(c_+^\dagger c_+ + c_-^\dagger c_- - d_+^\dagger d_+ - d_-^\dagger d_-)]^2 \rangle \\
&= (2b\hbar\bar{\omega}\tau/Mc)^2 \{ \langle (\Delta c_+^\dagger c_+)^2 \rangle + \langle (\Delta c_-^\dagger c_-)^2 \rangle + \langle (\Delta d_+^\dagger d_+)^2 \rangle + \langle (\Delta d_-^\dagger d_-)^2 \rangle \} \\
&= (2b\hbar\bar{\omega}\tau/Mc)^2 [4\hat{\beta}^2(\mu - \nu)^2 + 8(\mu\nu)^2] \\
&\approx (2b\hbar\bar{\omega}\tau/Mc)^2 [\hat{\beta}^2/\nu^2 + 8\nu^4] \text{ for } \nu \gg 1,
\end{aligned} \tag{74}$$

where we have used the orthogonality of the two different frequency modes in each interferometer arm, the unitary nature of (65), (66), and the assumed independent squeezed states for the transformed modes. Thus, combining (49), (53), (55), (72), and (74) we find that the total mean-square position error obeys

$$\begin{aligned}
\xi &= \text{SQL} [N_{CS}^{-1}(\hat{\beta}^2/2\nu^2 + 4\nu^4)(\bar{\omega}/\omega)^2 \\
&\quad + N_{CS}(\omega/16\omega_{IF})^2/2\hat{\beta}^2\nu^2].
\end{aligned} \tag{75}$$

Minimizing  $\xi$  over  $\nu^2$  and  $\hat{\beta}^2$  we obtain

$$\begin{aligned}
\xi_{\min} &= \text{SQL} N_{CS}^{-1/3} (\omega/2\omega_{IF})^{2/3} (\bar{\omega}/\omega)^2 \\
&\approx \text{SQL} N_{CS}^{-1/3} (\omega/2\omega_{IF})^{2/3}
\end{aligned} \tag{76}$$

with

$$\nu^2 = 8^{-1} (N_{CS}\omega/\omega_{IF})^{1/3}, \tag{77}$$

and

$$\hat{\beta}^2 = N_{CS}\omega/16\omega_{IF}, \tag{78}$$

corresponding to an average number of photons entering the interferometer given by

$$N_T = N_{CS}\omega/4\omega_{IF} + (N_{CS}\omega/\omega_{IF})^{1/3}/2. \tag{79}$$

Equation (76) shows that the two-frequency squeezed-state interferometer will substantially surpass<sup>15</sup> the SQL if  $N_{CS} > (\omega/2\omega_{IF})^2$ , e.g., for  $N_{CS} = 10^{20}$  and  $(\omega/2\omega_{IF}) = 10^7$  we find  $\xi_{\min} \approx 0.01$  SQL, with  $N_T \approx 10^7 N_{CS}$ . The sub-SQL performance requires an enormous increase in average photon number, plus a substantial added burden in system complexity to generate and heterodyne detect the two-frequency squeezed state fields. At this point, we should verify that the noise term we suppressed in (70) is, in fact, negligible. Assuming  $\delta l$  in  $B$  is on the order of  $\xi_{\min}^{1/2}$ , we find that this term will be smaller than the term we retained in (70) when  $\xi_{\min} < \text{SQL}$ . Indeed, for

$N_{CS} = 10^{20}$ ,  $(\omega/2\omega_{IF}) = 10^7$ , and  $\xi_{\min} = 0.01$  SQL, the neglected noise term is  $10^{-4}$  times the noise term we retained. Thus, our analysis is self-consistent.

Several concluding comments are now in order. The essence of the Shapiro and Wagner paper,<sup>3</sup> which underlies our two-frequency interferometer, is that there is no universal lower limit on phase uncertainty times amplitude uncertainty when measuring frequency beats via optical heterodyne detection. Thus, the performance shown in (76) comes about by using the squeezed states to simultaneously minimize radiation pressure fluctuations [cf. Eqs. (77)–(79) and Eqs. (6) and (7)], and make a squeezed phase-measurement on the intermediate-frequency signal [cf. Eqs. (50) and (72)]. Note that the behavior of our two-frequency interferometer would be quite different were we to assume that ideal photodetectors respond to energy flux instead of photon flux. In this case,<sup>13</sup> there is an intermediate-frequency uncertainty principle limiting simultaneous amplitude and phase measurements, from which it can be shown that the Fig. 3 interferometer achieves but does not exceed the SQL. As yet, the photodetector modeling issue is not fully resolved.

Finally, the Fig. 3 construction requires the mixed-frequency modes associated with the operators  $c_+$ ,  $c_-$ ,  $d_+$ , and  $d_-$  to be placed in independent squeezed states. It follows that the modes associated with  $a_+$  and  $a_-$  must be in correlated states, and likewise for  $b_+$  and  $b_-$ . The correlated modes for  $a_+$  and  $a_-$  may be generated, in principle, by use of a nearly degenerate parametric amplifier.<sup>14,16</sup>

#### ACKNOWLEDGMENTS

The authors acknowledge useful critical technical discussions with C. M. Caves. This research was supported by Office of Naval Research Contract No. N00014-81-K-0662.

<sup>1</sup>C. M. Caves, Phys. Rev. D **23**, 1693 (1981).

<sup>2</sup>H. P. Yuen, Phys. Lett. **56A**, 105 (1976).

<sup>3</sup>J. H. Shapiro and S. S. Wagner, IEEE J. Quantum Electron. **QE-20**, 803 (1984).

<sup>4</sup>H. P. Yuen, Phys. Rev. Lett. **51**, 719 (1983).

<sup>5</sup>H. P. Yuen, Phys. Rev. A **13**, 2226 (1976).

<sup>6</sup>H. P. Yuen and J. H. Shapiro, IEEE Trans. Inform. Theory **IT-26**, 78 (1980); see Ref. 3 for additional discussion of the heterodyne-detection case.

<sup>7</sup>W. H. Louisell, *Quantum Statistical Properties of Radiation*

(Wiley, New York, 1973).

<sup>8</sup>C. M. Caves, K. S. Thorne, R. W. P. Drever, V. D. Sandberg, and M. Zimmerman, Rev. Mod. Phys. **52**, 341 (1980).

<sup>9</sup>C. M. Caves, Phys. Rev. Lett. **45**, 75 (1980).

<sup>10</sup>The issue of nonclassical correlations in dual direct-detection systems has been discussed, in a different context, in M. S. Zubairy, Phys. Lett. **87A**, 162 (1982).

<sup>11</sup>P. Carruthers and M. M. Nieto, Rev. Mod. Phys. **40**, 411 (1968).

<sup>12</sup>R. Loudon, *The Quantum Theory of Light* (Oxford University

Press, Oxford, 1971), Chap. 7.

<sup>13</sup>The results of Ref. 3, and hence the remainder of Sec. V herein, depend critically on the fact that optical heterodyne detection is done with a photon detector rather than a power detector. See C. M. Caves, *Phys. Rev. D* **26**, 1817 (1982) for analysis of power-detector heterodyning. In particular, power-detector heterodyning yields an intermediate-frequency uncertainty principle which precludes simultaneous amplitude and phase measurements of arbitrary precision. We believe Caves's heterodyne analysis is not appropriate for the optical case, but is probably valid for microwave or radio frequency

heterodyning.

<sup>14</sup>The multimode two-photon coherent state of Ref. 3 is a notational translation of the multimode squeezed state of C. M. Caves, *Phys. Rev. D* **26**, 1817 (1982).

<sup>15</sup>Equations (75)–(79) supersede our preliminary report of an interferometer design surpassing the SQL contained in R. S. Bondurant and J. H. Shapiro, in *Coherence and Quantum Optics V*, edited by L. Mandel and E. Wolf (Plenum, New York, 1983), p. 629; the sub-SQL performance claimed therein is erroneous.

<sup>16</sup>B. L. Schumaker and C. M. Caves, in Ref. 15, p. 743.